BIOCELL
2019 43(2): 73-79

Tech Science Press

Mesenchymal stem cells are more effective than captopril in reverting cisplatin-induced nephropathy

Entsar A. SAAD[1]; Reda S. EL-DEMERDASH[2]; Eman M. ABD EI-FATTAH[1]

[1] Chemistry Department, Faculty of Science, Damietta University, Damietta, Egypt
[2] Urology & Nephrology Center, Faculty of Medicine, Mansoura University, Egypt

Key words: Histopathology, IL-10, Minerals, Nephropathy, Oxidative stress, PCR, Repair, TGF-β

Abstract: Cisplatin is a powerful anticancer drug but its nephrotoxic effects limit its clinical use. We aimed to evaluate the effect of mesenchymal stem cells (MSCs) injection or of captopril to counteract the cisplatin-induction of nephropathy. MSCs isolation, preparation and tracking, transforming growth factor-β (TGF-β) and interleukin-10 (IL-10) expressions, kidney function tests, oxidative stress state, and histological examinations were done. Cisplatin-induced nephropathy was indicated biochemically and confirmed histopathologically. MSCs treatment showed normal kidney architecture, and significantly decreased oxidative stress and TGF-β while increased IL-10 and improved kidney function tests. Rats treated with cisplatin + captopril showed noticeable kidney histopathological changes. Superior positive impact of MSCs in amelioration of cisplatin-induced nephropathy via their ability to motivate functional and structural renal repair is evidenced.

Introduction

Nephropathies may result as a consequence of chronic diseases, such as uncontrolled diabetes (Saad *et al*., 2015a), obesity (Habib *et al*., 2015) or cancer (Saad *et al*., 2017a), or may arise as a side effect of drugs such as cisplatin (Saad *et al*., 2017b) or as the result of exposure to toxicants (Saad, 2012; Saad, 2013; Toson *et al*., 2014). Inflammation and oxidative stress also aid in their development (Saad *et al*., 2017c).

Acute kidney injury (AKI) is a sudden decrease in kidney function. It is a serious clinical problem worldwide. In developing countries, 25-30% of hospital patients develop AKI. It affects about 11.3 million people and causes 1.4 million deaths annually (Rashid, 2017).

Cisplatin is an important chemotherapeutic drug used against many solid cancer tumors. It accumulates in kidney resulting in nephrotoxicity (Saad *et al*., 2017a; 2017b; 2017d) and leads to renal failure (Zaahkouk *et al*., 2015), which limits its clinical use. Many investigations introduced free radicals and oxidative stress as important contributors in cisplatin-induced nephrotoxicity and thereby in kidney cells degeneration (Zaahkouk *et al*., 2015). In general, cisplatin-induced nephrotoxicity is linked either to direct tubular toxicity, vascular factors, oxidative stress, or inflammation (Ahmed, 2014). As a consequence of these and for better clinical cancer treatment, researchers have two choices: either to develop new and safer alternatives to cisplatin, as in our recent published work (Saad *et al*., 2017a,b,d; Elsayed *et al*., 2018), or to look for new agents that can reduce or cancel cisplatin nephrotoxicity, to be administered along with cisplatin. One of the latter is captopril, an angiotensin-converting enzyme inhibitor, containing an -SH group which may be significant for its effectiveness (El-Sayed *et al*., 2008). Captopril may also act through locally decreasing TGF-β expression (De Albuquerque *et al*., 2004). Moreover, the use of stem cells capable of self-renewal and of producing subsequent generations with varying differentiation capabilities, are potentially useful to replace the damaged cells and tissues, with a lesser possibility of rejection and adverse effects (Saad *et al*., 2018a). In addition, it has been reported that treatment with exogenous mesenchymal stem cells (MSCs) during AKI might improve functional and structural recovery of renal compartments (Asanuma *et al*., 2010). Thus, we here aimed to compare the effect of a single injection of MSCs with the effect of oral captopril administration for consecutive 15 days, on cisplatin-induced nephropathy in rats.

Material and Methods

Isolation and preparation of bone marrow-derived MSCs
Sprague-Dawley male rats (12-weeks old) were anesthetized and the skin was sterilized with ethanol (70%) then the

*Address correspondence to: Entsar A. SAAD, entsarsaad@gmail.com

DOI: 10.32604/biocell.2019.07020

femurs and tibia were separated and immersed in ethanol (70%) for two minutes. The bones were washed using phosphate buffered saline (Hyclone, USA). Then the bone marrow was extracted from the bones in a laminar air flow cabinet; after removal of the two ends of the bones, bone marrow was cropped by flushing the tibiae and femurs with Dulbecco's modified Eagles medium (DMEM) (Lonza, Belgium) supplemented with 10% fetal bovine serum and 1% penicillin/streptomycin. The marrow plugs were grown in 20 mL complete media and incubated in 5% humidified CO_2 incubator at 37°C for 7-10 days as a primary culture. Cells were examined daily with an inverted microscope, to follow up their growth. MSCs were distinguished from other bone marrow cells by their ability to adhere to tissue culture polystyrene flask. At the end of the expansion phase, the MSCs became homogenous, spindle shaped, fibroblast-like and arranged in monolayer (Fig. 1). MSCs cells were counted using trypan blue. To track MSCs tissue distribution and localization (Fig. 1), they were labeled using Qtracker® 655 cell labeling kit, according to the manufacturer's instructions (Thermo Fisher Scientific, https://www.thermofisher.com).

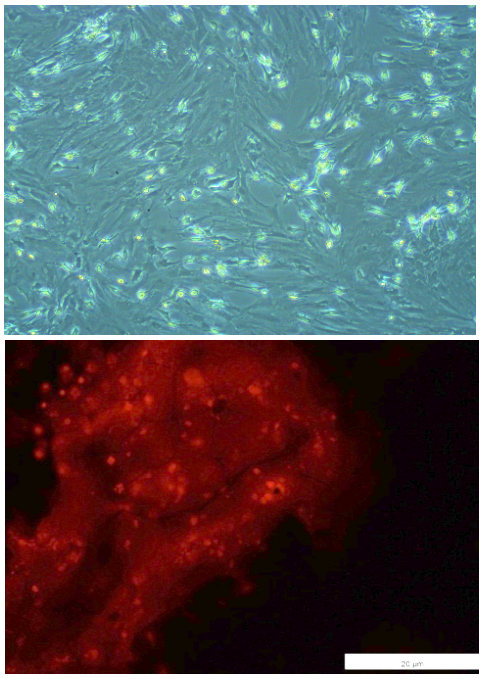

FIGURE 1. Morphology of mesenchymal stem cells (MSCs), ten days after isolation (x100) showing spindle shape fibroblast-like cells. Immuno-fluorescent labeling of MSCs; Qtracker-positive MSCs with red fluorescence detected in kidney tissue.

Animals and experimental design

Fifty male albino rats (Sprague-Dawley strain), 12-weeks old and weighing 180-230 g, were obtained from the Animal House of Nile Center for Experimental Researches, Mansoura, Egypt. They were housed (four rats per cage) according to guidelines of National Institute of Health (NIH, 1996), under standardized laboratory conditions with controlled light/dark cycle, temperature of 22 ± 2°C and moisture of 60-70%. Animals had normal food and water supply *ad libitum*. Rats were divided into five equal groups, 10 rats each:

Group 1 (Control): injected i.p. with 1 mL saline.

Group 2 (Sham): injected i.v. with 0.2 mL DMEM.

Group 3 (Cisplatin): injected i.p. with a single dose of cisplatin (6 mg/kg).

Group 4 (Cisplatin + MSCs): injected i.p. with a single dose of cisplatin (6 mg/kg) followed after 3 days by i.v. injection of MSCs single dose (1.2×10^6 cells /rat).

Group 5 (Cisplatin + captopril): injected i.p. with a single dose of cisplatin (6 mg/kg) followed after 3 days by captopril administration (100 mg/kg/orally/day) for 15 consecutive days.

All rats were sacrificed 21 days after cisplatin injection. The experimental protocol was approved by Chemistry Department, Faculty of Science, Damietta University, Egypt.

Samples

Rats were fasted overnight and sacrificed under light ether anesthesia. Blood was collected by cardiac puncture. Sera were separated by centrifugation at 3000 rpm for 20 minutes and stored in small aliquots at -20°C for further analysis. Kidney tissues were quickly removed and rinsed with sterile cold isotonic saline solution (0.9%). Each kidney sample was divided into three parts: one part was homogenized, centrifuged and the resulting homogenate was stored at -20°C for determination of renal total antioxidant capacity (TAC) and malondialdehyde (MDA). The other 2 parts were separately fixed in 10% formalin; one of them was used for the histopathological examination and the other was used for kidney examination using fluorescent microscopy to show the Qtracker reagent distribution in the cytoplasm of the MSCs.

Biochemical examinations

Kidney tissues concentrations of MDA and TAC were determined using kits supplied by Biodiagnostic Company (Cairo, Egypt). Serum creatinine levels were determined following instructions of creatinine kit supplied from Beckman (USA). Uric acid, blood urea nitrogen (BUN), total cholesterol and triglycerides serum concentrations were determined according to their kits obtained from Spinreact (St. Esteve d'en Bas Girona, Spain). Serum urea concentration was determined using urea kit from Diamond Company (Cairo, Egypt). Serum albumin and total proteins were determined by kits from Egyptian American Company for Laboratory Services (Egypt). Serum phosphorus content was estimated using Lab-Care Diagnostics (INDIA) kit. Serum potassium and sodium contents were determined using Spectrum, Egyptian Company for Biotechnology, Egypt kits. Real-time PCR was used to measure expression of mRNAs of TGF-β and IL-10 genes in kidney tissue against β-actin as an internal reference. Used forward and reverse primers are recorded in Tab. 1. All biochemical assays were done in duplicate.

Histopathological examination

Fixed kidney tissues in 10% formalin were dehydrated via graded series of ethanol (50-100%) and cleared in xylene. Infiltrated tissues were then embedded into paraffin wax. Transverse sections of kidney (5 µm thick) were obtained and stained with Mayer's hematoxylin and eosin, and then blindly examined by a pathologist.

TABLE 1

Forward and reverse primers

Gene	Forward primer (′5 ------ ′3)	Reverse primer (′5 ------ ′3)	Sequence ID
Transforming growth factor-β (TGF-β)	CCTGCAAGACCATCGACATG	GCGAGCCTTAGTTTGGACAG	NM_021578.2
Interleukin-10 (IL-10)	GTTGCCAAGCCTTGTCAGAA	CCTTGATTTCTGGGCCATGG	NM_012854.2
β-actin	CACCATGTACCCAGGCATTG	CACACAGAGTACTTGCGCTC	NM_031144.3

Statistical analysis

All values are presented as mean ± SEM. Differences were considered significant at $p < 0.05$ (one-tailed). One-way analysis of variance (ANOVA) and post-hoc test were employed to calculate differences between groups. The SPSS/PC program (version 17; SPSS, Chicago, Illiniois, USA) was used for statistical analysis.

Results

The sham group did not show any significant change compared to control group at both histological and biochemical levels.

After cisplatin injection to normal rats serum biochemical markers for kidney damage were significantly increased; creatinine and urea were increased for more than 3-folds, and uric acid and BUN for more than 2-folds. Treatment with MSCs significantly decreased serum creatinine and urea by 50%, and uric acid and BUN by about 27% and 36%, respectively. Treatment with captopril also decreased significantly these kidney damage indicators but the percent decreases were much lower than those induced by MSCs treatment (Tab. 2).

Serum phosphorus concentration was significantly increased while potassium and sodium concentrations were decreased in rats with cisplatin-induced renal damage. Phosphorus, sodium and potassium levels were significantly reversed towards normality by both MSCs and captopril treatments (Fig. 2).

Comparing to control, cholesterol and triglycerides levels in sera of cisplatin-treated rats were nearly doubled, whereas albumin levels were reduced by about 75% and total proteins levels were reduced by 50%. All these differences were statistically significant. When MSCs were injected to cisplatin treated-rats, cholesterol and triglycerides levels were significantly decreased by 29% and 26%, respectively while albumin and total proteins levels were significantly increased by 129% and 60%, respectively. A similar trend was observed when captopril was administered to cisplatin-treated rats but MSCs effect was better (Tab. 3).

TABLE 2

Serum creatinine, uric acid, blood urea nitrogen (BUN) and urea levels in different rat groups

Groups	Creatinine (mg/dL)	Uric acid (mg/dL)	BUN (mg/dL)	Urea (mg/dL)
Control	0.77 ± 0.03	3.81 ± 0.05	10.01 ± 0.1	25.17 ± 0.14
Sham	0.93 ± 0.02	3.85 ± 0.05	10.14 ± 0.16	25.25 ± 0.15
Cisplatin	2.68 ± 0.09***	8.06 ± 0.07***	26.09 ± 0.16***	86.21 ± 0.64***
Cisplatin + MSCs	1.31 ± 0.07***,†††,‡	5.92 ± 0.17***,†††	16.51 ± 0.23***,†††,‡	43.06 ± 1.46***,†††
Cisplatin + Captopril	1.57 ± 0.09***,†††	6.28 ± 0.16***,†††	17.22 ± 0.33***,†††	43.47 ± 1.66***,†††

Data are expressed as mean ± SEM. n=10 for each group. *** is $p < 0.001$ compared to control group. ††† is $p < 0.001$ compared to cisplatin group. ‡ is $p < 0.05$ compared to cisplatin + captopril group.

TABLE 3

Serum cholesterol, triglycerides, albumin and total protein in different rat groups

Groups	Cholesterol (mg/dL)	Triglycerides (mg/dL)	Albumin (g/dL)	Total protein (g/dL)
Control	58.41 ± 2.12	72.01 ± 1.81	4.56 ± 0.13	8.36 ± 0.19
Sham	55.83 ± 2.44	68.72 ± 2.15	4.51 ± 0.15	8.52 ± 0.18
Cisplatin	107.09 ± 4.66***	127.53 ± 4.46***	1.19 ± 0.09***	4.15 ± 0.19***
Cisplatin + MSCs	75.87 ± 2.06***,†††,‡‡	95 ± 3.21***,†††,‡‡	2.73 ± 0.17***,†††,‡‡	6.62 ± 0.21***,†††,‡‡
Cisplatin + Captopril	89.48 ± 2.4***,†††	103.51 ± 3.42***,†††	2.13 ± 0.15***,†††	5.7 ± 0.15***,†††

Data are expressed as mean ± SEM. n = 10 for each group. *** is $p < 0.001$ compared to control group. ††† is $p < 0.001$ compared to cisplatin group. ‡‡ and ‡‡‡ are $p < 0.01$ and $p < 0.001$, respectively compared to cisplatin + captopril group.

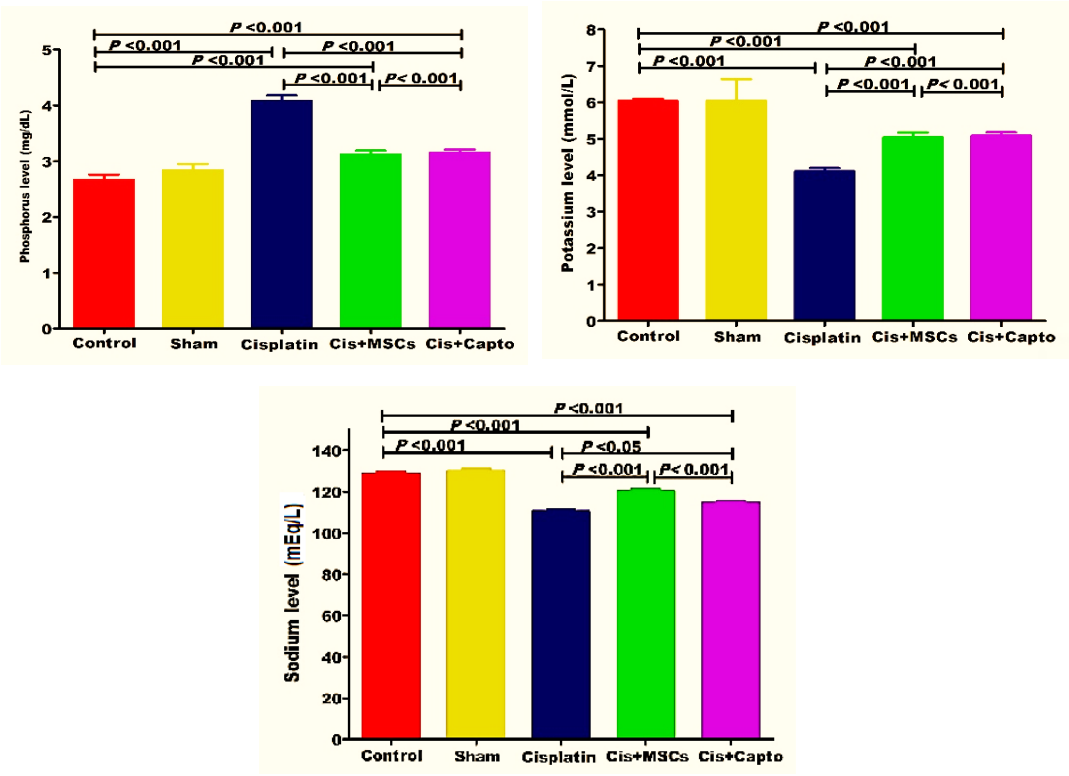

FIGURE 2. Phosphorus, potassium and sodium serum levels in different groups. Data are expressed as mean ± SEM; n = 10 per group.

Rats treated with cisplatin showed significantly higher peroxidation as evidenced by more than a 5-fold increase in renal MDA, with a 44% decrease in TAC, as compared to control. Treatment of cisplatin-treated rats with MSCs exhibited a significant reduction in oxidative stress, represented by 48% decrease in MDA and 25% increase in TAC, while treatment with captopril lowered MDA levels by only 28% and increased TAC by only 19% (Tab. 4).

As illustrated in Fig. 3, TGF-β gene expression was increased by more than 5-folds in cisplatin-treated group, as compared with the control group, while it was decreased by about 50% in the group that received MSCs, and by more than 50% in the group that received captopril. On the other hand, IL-10 gene expression was decreased by 87% in cisplatin-treated group, as compared to control group, whereas it was increased by 392% in the group that received MSCs. A smaller effect was observed in the group that received captopril. Again, all the mentioned differences were statistically significant.

Fig. 4 showed kidney histopathological changes in the different groups. Cisplatin treatment induced extensive tubular necrosis, associated with calcification and epithelial dysplasia in the remaining renal tubules. Captopril treatment resulted in a partial reversal of cisplatin-induced nephropathy, with still noticeable tubular necrosis and periglomerular and peritubular fibrosis and infiltration. In turn, MSCs treatment effectively reversed the cisplatin-induced nephropathy.

TABLE 4

Renal malondialdehyde (MDA) and total antioxidant capacity (TAC) in different rat groups

Groups	MDA (nmol/g tissue)	TAC (μmol/L)
Control	31.02 ± 1.13	1.14 ± 0.03
Sham	26.04 ± 1.27	1.15 ± 0.03
Cisplatin	164.18 ± 16.17***	0.79 ± 0.03***
Cisplatin + MSCs	87.67 ± 8.65***,†††,‡‡	0.99 ± 0.02***,†††,‡
Cisplatin + Captopril	117.53 ± 5.08***,†††	0.94 ± 0.02***,††

Data are expressed as mean ± SEM. n = 10 for each group. *** is $p < 0.001$ compared to control group. †† and ††† are $p < 0.01$ and $p < 0.001$, respectively compared to cisplatin group. ‡ and ‡‡ are $p < 0.05$ and $p < 0.01$, respectively compared to cisplatin + captopril group.

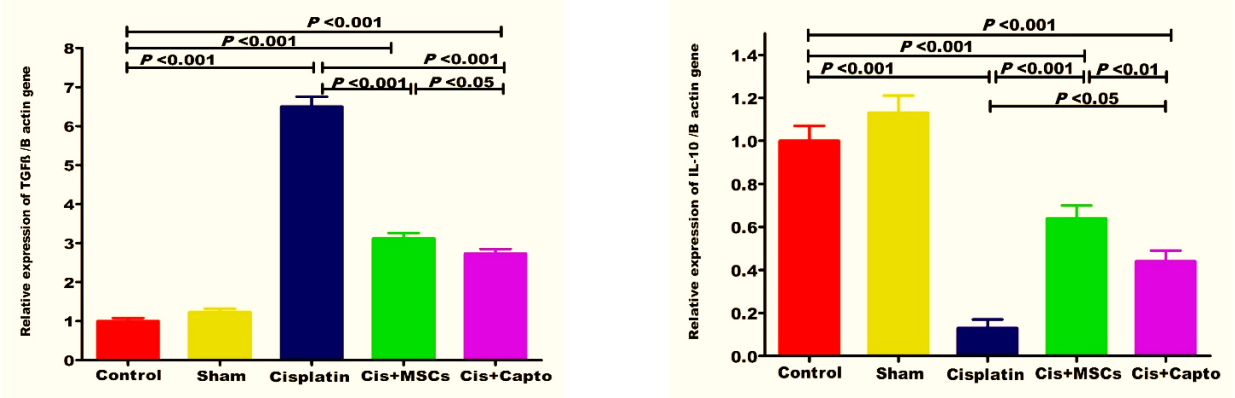

FIGURE 3. Real-time quantitative PCR analysis of the expression of transforming growth factor beta (TGF-β) and interleukin-10 (IL-10) genes in kidney tissue in cisplatin (cis)-induced kidney damage in rats after treatment by mesenchymal stem cells (MSCs) or by capatopril (capto). Data are expressed as mean ± SEM; n = 10 per group.

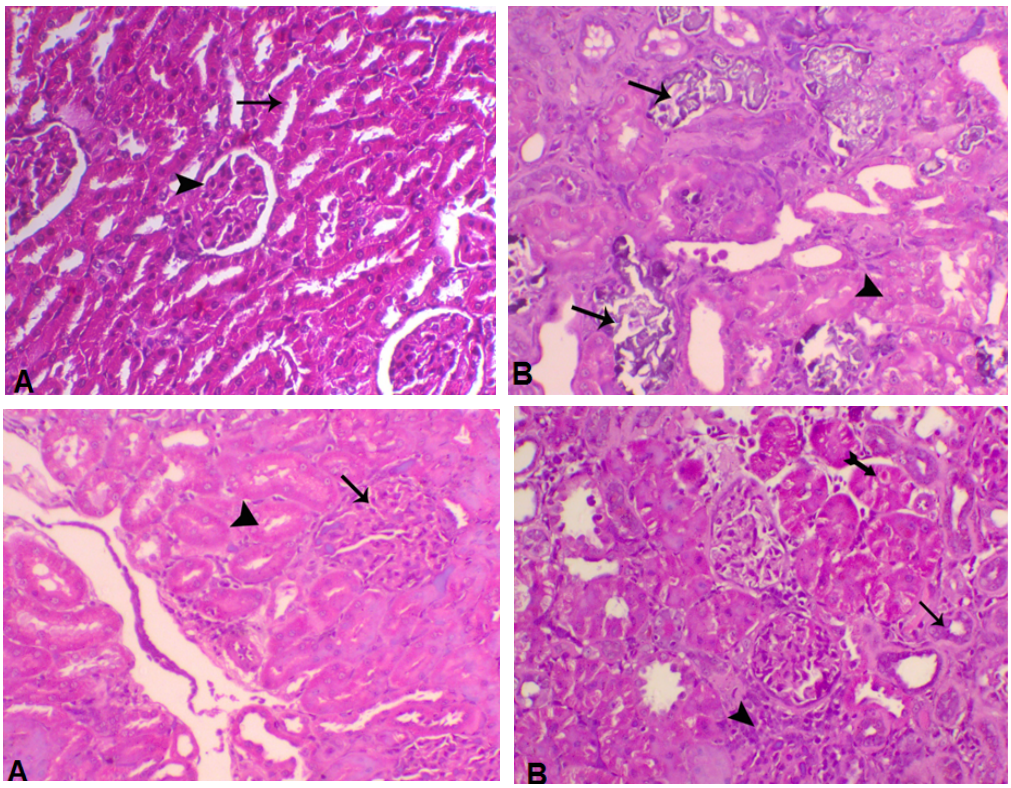

FIGURE 4. Histopathology (hematoxylin and eosin, X200) of control and treated kidneys. Control kidney showing normal renal tubules (arrow) and glomeruli (arrowhead) (**A; up**), cisplatin-treated kidney showing extensive necrosis of renal tubules associated with calcification (arrow) and dysplasia within the other renal tubules (arrowhead) (**B; up**). Kidney of rat treated with cisplatin + MSCs showing renal tubules (arrowhead) and glomeruli (arrow) within the normal limits (**A; down**), kidney of rat treated with cisplatin + captopril showing noticeable necrosis of renal tubules (tailed arrow), periglomerular and peritubular fibrosis and infiltration (arrowhead), and regeneration of some renal tubules (arrow) (**B; down**).

Discussion

In the present study, kidney dysfunction in our rat cisplatin-induced nephropathy model was indicated by high circulated levels of creatinine (> 3-fold), urea (> 3-fold), uric acid (> 2-fold), and BUN (> 2-fold) associated with more than 5-fold increase in MDA level accompanied by 44% decrease in antioxidant defense power (TAC) in the renal tissue following cisplatin injection. Similar findings were observed by preceding workers (Maheshwari *et al.*, 2013; Saad *et al.*, 2018b,c). Our histopathological data added another confirmation for the aforementioned renal failure, via detection of extensive necrosis of renal tubules, that was associated with renal tubules calcification and/or dysplasia. These observations are in agreement with those of Zaahkouk *et al.* (2015). In fact, these findings indicate that the main cause behind cisplatin-induced nephropathy may the high increase in lipid peroxidation, resulting in an imbalance with the antioxidant defense system suppression, and consequent renal tissue damage.

In the current work and in agreement with Launay-Vacher *et al.*, 2008, cisplatin-induced nephropathy was

accompanied by high serum phosphorus and low serum potassium and sodium concentrations. These disturbances may be attributed to abnormal transport system during acute renal failure state.

Moreover, serum cholesterol and triglycerides levels of cisplatin-treated rats were nearly doubled. Hepatic damage has been also shown by liver function tests (Saad, 2014; Saad and Habib, 2013; Saad *et al*., 2015b; Saad *et al*., 2017e). In this work, serum albumin was decreased by about 75% and total proteins were reduced to 50%, which also suggest hepatic damage (Attallah *et al*., 2015; El-Emshaty *et al*., 2018) provoked by cisplatin-induced oxidative stress. Albumin decrease may also be explained by excessive renal excretion induced by cisplatin toxicity. Reduced albumin level was previously described by Alam and Vijayanarayana (2013).

The present study confirms cisplatin ability to cause renal tubular severe injury, associated with peritubular fibrosis. Accordingly, a more than 5-fold overexpression of TGF-β, the major fibrogenic cytokine, has been observed here as a consequence of cisplatin treatment. These findings are similar to those of Bonventre (2014) and Nagaishi *et al*., (2016). Furthermore, cisplatin was able to down-regulate the anti-inflammatory cytokine IL-10 expression in renal tissues, perhaps through the cytotoxic effect of this drug on white blood cells. This is in harmony with the report of Omata *et al*., (1996).

Due to the mesenchymal origin of nephrons and the crucial value of stromal cells signaling for the development of nephrons and collecting ducts, MSCs have been strongly recommended for repairing kidney damage (Anglani *et al*., 2004). In the present study, Qtracker-marked MSCs were found in the damaged kidney after systemic injection (Fig. 1) and triggered secretion of IL-10, an anti-inflammatory marker. Besides that, they seemingly differentiated into new renal cells, as shown by the histopathological recovery of the cisplatin-induced changes (Fig. 4). The histopathological recovery was accompanied by (1) a lowering of MDA and an augmentation of TAC; (2) a decrease in TGF-β expression; (3) decreases in serum creatinine and urea, BUN and uric acid. Moreover, serum phosphorus, sodium, potassium, cholesterol, triglycerides, albumin and total proteins levels were reversed towards normality. These findings are consistent with those of Nagaishi *et al*., 2016 in mice, and indicate that MSCs treatment is much more effective than captopril in reversing the effects of cisplatin-induced nephropathy.

Acknowledgement

The study originates from a master thesis. This work was done by all authors cooperatively.

Conflict of Interest

Authors have no conflict of interest regarding this study.

References

Ahmed LA (2014). Renoprotective effect of Egyptian cape gooseberry fruit (*Physalis peruviana L.*) against acute renal injury in rats. *The Scientific World Journal,* Article ID 273870, 7 pages.

Alam Q, Vijayanarayana K (2013). Nephroprotective effect of alcoholic extracts of fruits of *Solanum xanthocarpum* against cisplatin-induced nephropathy in rats. *International Journal of Advances in Pharmacy, Biology and Chemistry* **2**: 147-151.

Anglani F, Forino M, Prete DD, Tosetto E, Torregrossa R, D'Angelo A (2004). In search of adult renal stem cells. *Journal of Cellular and Molecular Medicine* **8**: 474-478.

Asanuma H, Meldrum DR, Meldrum KK (2010). Therapeutic applications of stem cell to repair kidney injury. *Journal of Urology* **184**: 26-33.

Attallah A, El-Far M, Abdel Malak C, Omran M, Farid K, Yahya R, Saad EA, Albannan MS, Attallah AA, El Basuni MA, Ali IS, Abed SB, El Naggar MA (2015). A simple diagnostic index comprising epithelial membrane antigen and fibronectin for hepatocellular carcinoma. *Annals of Hepatology* **14**: 869-880.

Bonventre JV (2014). Primary proximal tubule injury leads to epithelial cell cycle arrest, fibrosis, vascular rarefaction, and glomerulosclerosis. *Kidney International Supplements* **4**: 39-44.

De Albuquerque DA, Saxena V, Adams DE, Boivin GP, Brunner HI, Witte DP, Singh RR (2004). An ACE inhibitor reduces Th2 cytokines and TGF-β1 and TGF-β2 isoforms in murine lupus nephritis. *Kidney International* **65**: 846-859.

El-Emshaty HM, Saad EA, Gouida MS, Elshahawy ZR (2018). Associations between CD133, CK19 and G2/M in cirrhotic HCV (genotype-4) patients with or without accompanying tumor. *Biocell* **42**: 55-60.

El-Sayed M, Abd-Ellah MF, Attia SM (2008). Protective effect of captopril against cisplatin-induced nephrotoxicity in rats. *Pakistan Journal of Pharmaceutical* Sciences **21**: 255-261.

Elsayed SA, Saad EA, Mostafa SI (2019). Development of new potential anticancer metal complexes derived from 2-Hydrazinobenzothiazole. *Mini-Reviews in Medicinal Chemistry* **19**: 913-922.

Habib S, Saad EA, Elsharkawy AA, Attia ZR (2015). Pro-inflammatory adipocytokines, oxidative stress, insulin, Zn and Cu: interrelations with obesity in Egyptian non-diabetic obese children and adolescents. *Advances in Medical Sciences* **60**: 981-971.

Launay-Vacher V, Rey JB, Isnard-Bagnis C, Deray G, Daouphars M (2008). Prevention of cisplatin nephrotoxicity: state of the art and recommendations from the European Society of Clinical Pharmacy Special Interest Group on Cancer Care. *Cancer Chemotherapy and Pharmacology* **61**: 903-909.

Maheshwari RA, Sailor GU, Patel L, Balaraman R (2013). Amelioration of cisplatin-induced nephrotoxicity by statins. *Indian Journal of Pharmacology* **45**: 354-358.

Nagaishi K, Mizue Y, Chikenji T, Otani M, Nakano M, Konari N, Fujimiya M (2016). Mesenchymal stem cell therapy ameliorates diabetic nephropathy via the paracrine effect of renal trophic factors including exosomes. *Science Reports* **6**: 34842.

Omata K, Kanazawa M, Sato T, Abe F, Saito T, Abe K (1996). Therapeutic advantages of angiotensin converting enzyme inhibitors in chronic renal disease. *Kidney International* **49**: S57-S62.

Rashid HU (2017). Acute kidney injury-recent thoughts in diagnosis and management. *Journal of Urology* & *Nephrology* **2:** 000113.

Saad EA (2012). Curative and protective effects of L-arginine on carbon tetrachloride-induced hepatotoxicity in mice. *Biochemical and Biophysical Research Communications* **423**: 147-151.

Saad EA (2013). Kidney response to L-arginine treatment of carbon tetrachloride-induced hepatic injury in mice. *Natural Science* **5**: 1-6.

Saad EA (2014). Non-invasive assessment of liver fibrosis using serum markers. *Journal of Pharmaceutical, Chemical and Biological Sciences* **2**: 59-76.

Saad EA, El-Gayar HA, EL-Demerdash RS, Radwan KH (2018b).

Hepato-toxic risk of gum arabic during adenine-induced renal toxicity prevention. *Journal of Applied Pharmaceutical Science* **8**: 104-111.

Saad EA, El-Gayar HA, EL-Demerdash RS, Radwan KH (2018c). Frankincense administration antagonizes adenine-induced chronic renal failure in rats. *Pharmacognosy Magazine* **14**: 634-640.

Saad EA, Habib SA (2013). Effect of crude extracts of some medicinal plants on the osmotic stability of human erythrocytes *in vitro*. *Journal of Free Radicals and Antioxidants Photon* **139**: 265-272.

Saad EA, Habib SA, Eltabeey M (2017e). Diagnostic performance of AFP, autotoxin and collagen IV and their combinations for non-invasive assessment of hepatic fibrosis staging in liver fibrosis patients associated with chronic HCV. *International Journal of Pharmaceutical Quality Assurance* **8**: 165-173.

Saad EA, Habib SA, Refai WA, Elfayoumy AA (2017c). Malondialdehyde, adiponectin, nitric oxide, C-reactive protein, tumor necrosis factor-alpha and insulin resistance relationships and inter-relationships in type 2 diabetes early stage. Is metformin alone adequate in this stage? *International Journal of Pharmacy and Pharmaceutical Sciences* **9**: 176-181.

Saad EA, Hassanien MM, El-Hagrasy MA, Radwan KH (2015a). Antidiabetic, hypolipidemic and antioxidant activities and protective effects of *Punica granatum* peels powder against pancreatic and hepatic tissues injuries in streptozotocin induced IDDM in rats. *International Journal of Pharmacy and Pharmaceutical Sciences* **7**: 397-402.

Saad EA, Hassanien MM, El-lban FW (2017a). Nickel(II) diacetyl monoxime-2-pyridyl hydrazone complex can inhibit Ehrlich solid tumor growth in mice: a potential new antitumor drug. *Biochemical and Biophysical Research Communications* **484**: 579-585.

Saad EA, Hassanien MM, El-mezayen HA, ELmenawy NM (2017b). Regression of murine Ehrlich ascites carcinoma using synthesized cobalt complex. *Medicinal Chemistry Communication* **8**: 1103-1111.

Saad EA, Hassanien MM, Elneely EA (2017d). Iron(III) diacetylmonoxime-2-hydrazinopyridine complex: a new prospective antitumor drug. *Applied Organometallic Chemistry* **31**: e3684.

Saad EA, Marei HES, El-Magd MA, El-Fatiry HM (2018a). Molecular characterization of olfactory bulb neural stem cells during proliferation and differentiation. *Journal of Applied Pharmaceutical Science* **8**: 87-92.

Saad EA, Toson E, Ahmed G (2015b). Clove or green tea administration antagonizes khat hepatotoxicity in rats. *International Journal of Pharmacy and Pharmaceutical Sciences* **7**: 72-76.

Toson EA, Habib SA, Saad EA, Harraz NH (2014). Toxic and anti-fertility effects of *Alocasia macrorrhiza* and *Calotropis procera* ethanolic extracts on male mice. *International Journal* of *Biochemistry Photon* **195**: 328-338.

Zaahkouk SMA, Bakry S, Mansour A, Ibrahim RH (2015). Therapeutic role of mesenchymal stem cells in cisplatin induced renal failure in adult male rats. *Advances in Biological Research* **9**: 201-209.